EFFECT OF MINERAL SYSTEMS ON LEAD REMOVAL FROM AQUEOUS SOLUTION PART I

Davidson Egirani
(Corresponding Author)
Niger Delta University
NIGERIA

Napoleon Wessey
Niger Delta University
NIGERIA

Adedotun Aderogna
Niger Delta University
NIGERIA

ABSTRACT

Mineral systems have been investigated to determine their effect on lead removal. These mineral systems comprises kaolinite, montmorillonite, goethite and their mixtures. This study was in relation to reactivity and kinetics relevant to streams and groundwater impacted by lead. The batch mode study was conducted at room temperature (23 ± 2 ◦C). Reactivity studies demonstrate enhancement of proton coefficient and the acidity of reactive sites by mixed mineral systems except for kaolinite-montmorillonite, thus increasing lead removal by proton exchange. Kinetic studies demonstrate two- phase reactions with minimal intra-particle diffusion attributed to outer sphere complexation and inner sphere complexation. In the first-phase reaction, mineral mixing decreased the mass transfer rates for kaolinite-montmorillonite and montmorillonite-goethite, not affecting kaolinite-goethite. For the second-phase reaction, mineral mixing did not change the mass transfer rates for the mixed mineral systems except for montmorillonite-goethite. The behaviors of the mixed mineral systems suggest that different reactive sites were involved at the onset of sorption, with reactions and sorption ending with inner-sphere complexation.

Keywords: Particle size, lead, removal, kinetics, mixed mineral systems.

INTRODUCTION

As a common heavy metal, lead has been used as raw material in the production of pigments for lead paints, but its toxic properties for human health and ecosystem have attracted increasing attention [Zhao et al., 2013], [Eric, et al., 2010, Stephan, et al., 2010],[Dastoora, et al., 2004, [Deshicar, et al., 1990], 13].Technologies involved in heavy metal removal from aqueous solution have been reviewed by several workersElouear, et al., 20084]. Among the different treatments described, adsorption technology is attractive due to its merits of efficiency, economy and simple operation [Crini, 2005] .For adequate treatment of water containing lead using mineral systems, reactivity and the kinetic reaction partners to the reactive sites of sorbents is required [Dzombak and Morel, 1990, Lopez-Mu˜noza, et al., 2011]. Lead removal from aquatic systems is measured by the speciation, mobility, particle size, sorbent surface charge, surface area of the mineral sorbent, solution dilution and H+/ − M exchange stoichiometry [Hatje, et al., 2003, Reichenberg, 1952]. The aim of this study is to explore the effect of particle size of single and mixed mineral systems of kaolinite-montmorillonite, kaolinite-goethite and montmorillonite-goethite on sorption behavior of lead in relation to reactivity and removal kinetics. Different kinetic models have been applied to validate sorption mechanism.

Theoretical Models and Isotherms

Distribution coefficient (Kd) was used in this paper as provided elsewhere [O¨ zcan et al., 2006], [Egirani et al., 2005a], [Tombacz et al., 1999]. Kd(L/kg) was calculated from the Freundlich model equation,

$S = KdC^N$ (1)

where S is the sorbed concentration (µg/kg), Kd is the distribution coefficient, C is the equilibrium concentration (µg/l), and N = 1 is a chemical-specific coefficient derived from the slope of the plot. The empirical model to address the mineral-Pb interactions is given:

$$Kd_{total} = \frac{Kd_1 + Kd_2 + Kd_n}{n} \quad (2)$$

Where Kd total is the theoretical distribution coefficient for a 1:1 mixed suspension, Kd1 is the distribution coefficient for first single mineral suspension, and Kd_2 is the distribution coefficient for second single mineral suspension, Kdn is the distribution coefficient for n number of mineral suspensions and n is the number of mineral suspensions.

Lead removal. Mineral mixing is said to (a) enhances Hg removal where the difference is positive; (b) attenuate Hg removal where the difference is negative; and (c) have no effect on lead removal where no difference exist between the actual Kd and theoretical Kd:

$$\Delta Kd = Kd - Kd_{total} \quad (3)$$

$$\Delta\alpha = \alpha - \alpha_{total} \quad (4)$$

$$\Delta K_f = K_f - K_{f\ total} \quad (5)$$

Where α, K_f α_{total} and $K_{f\ total}$

Is the proton coefficient, mass transfer rate?
Theoretical proton coefficient and theoretical mass transfer coefficient, respectively.

Mass Balance and Kinetics

The mass balance of Pb(II) sorbed per unit mass of the mixed mineral suspension (mg/g) was calculated by the following [Blesa, et al., 1997], [McBride 1982]:

$$Q_e = \langle Ci - Ce \rangle \frac{V}{W} \quad (6)$$

Where Ci and Ce are the initial and equilibrium Pb(II) concentrations in mg/L, V is volume of the Pb(II) solution in ml, and W is the weight of adsorbent in mg respectively.

The transport of adsorbate from external layers to the mineral surface where sorption occurs is dependent on a mass transfer constant Kf obtained from the slopes of the curve derived from plotting Ct/C0 vs time.

$$\left[\frac{d(C_t/C_0)}{dt}\right]_{t=0} \cong -K_f Ss \quad (7)$$

Where Ct and C0 are the initial concentrations of Pb(II) at time t, Ss is the exposed external surface area of the sorbent, and Kf is the mass transfer coefficient [Al-Degs, et al., 2003]. The Freundlich isotherm was chosen to describe sorption of Pb(II) because this is suitable for heterogeneous surfaces over a wide range of solute concentrations [Venegas et al., 2008]. To gain insight into the mechanisms and rate controlling steps affecting the kinetics of adsorption, Bangham kinetic model was [Feng et al., 2004]:

$$Q_t = k_i t^{0:5} + C \quad (8)$$

Where ki is the intraparticle diffusion constant (mg/g min) and the intercept (C) reflects the boundary layer effect. The values of ki are calculated from slopes (ki) of the plots of qt vs. t0.5. The plot of qt vs. t0.5 should be linear if intra-particle diffusion is involved in the adsorption process and if these lines pass through the origin then intraparticle diffusion is the rate controlling step. When the plots do not pass through the origin, this is indicative of some degree of boundary layer control and further shows that the intraparticle diffusion is not the only rate limiting step, but also other kinetics models may control the rate of adsorption, all of which may be operating simultaneously.

LITERATURE REVIEW

There are literature reviews to evaluate the effectiveness of locally sourced materials in remediation of contaminated waters and soils [Kitano, et al., 1980, Ravichandran, 2004]. [22]. Also, several methods have been established in heavy metal treatment in contaminated water [Tan et al., 2011, Olivaa, et al., 2011, Luo et al., 2013, Wang et al., 2013], Anagnostopoulos et al., 2012]. Some literatures have reviewed the technologies for removing lead in aqueous solution [Cataldo et al., 2013] and the effect of particle size on metal sorption [Strange and Onwulata,, 2002, Eze, et al., 2013]. However, some of these new techniques are have limited applications and the reactivity and removal kinetics require further investigation. Therefore, innovative cost-effective treatment processes are urgently needed. One of such emerging method is the use of mixed mineral systems of clays and hydroxide(s).

METHODOLOGY

Characterization

Richard Baker Harrison Company and Acros Organics Ltd. provided the mineral systems used in this study. An aqueous solution of Pb was prepared at variable concentrations from its nitrate salt. .Lead nitrate $Pb(NO3)_2$ provided by Iconofile Company Inc was employed as the source of Pb(II) .A standard solution containing variable concentrations of Pb(II) in ppm was prepared by dissolving $PbCl_2$ (Merck) in distilled water.

Table1: Characteristics of Mineral Systems

Mineral systems	Particle size range (μm)			% (<1 μm) colloid	pH ± σ	Surface area(SSA±σ) (m2/g)
K	15-30	30-45	45-60	3.00	6.05±0.05	47.01± 0.24
M	15-30	30-45	45-60	0.53	.01±0.09	10.00± 0.00
G	25-50	50-75	75-100	2.92	8.05±0.06	71.05± 0.17
K M	15-30	30-45	45-60	0.97	5.01±0.02	88.05± 0.55
MG	1-4	4-8	8-12	3.85	3.03± 0.04	147.10± 0.50
KG	25-50	50-75	75-100	0.73	3.05± 0.01	79.30± 0.59

In this section of the report, K, M, G, KM, MG and KG represents kaolinite, montmorillonite All experimental studies were conducted in triplicates and samples were stored in the dark at room temperature (23±3 ◦C) not exceeding 24 h before analysis [45]. Supernatant was filtered through a cellulose acetate filter (pore size 0.2μm) and analyzed for Pb(II) using a Hitachi Atomic Absorption Spectrophotometer (HG-AAS). The working solutions of different concentrations were prepared by diluting the stock solution immediately before starting the batch studies. Mineral systems were characterized using Coulter laser method to determine the particle sizes. % colloid was estimated from the particle size distribution curves. Equilibrium pH of the untreated mineral suspensions was determined using the Model 3340 Jenway ion meter. The standard volumetric Brunauer, Emmett, and Teller (BET) method was used to determine the surface areas [Brunauer, et al., 1938], [Hlavay, et al., 2005]. Spectral analysis was performed using scanning electron microscopy (SEM) and energy dispersive spectroscopy (EDS) to confirm the mineral sorbent[Hlavay, 1993], [Egirani, et al., 2005b]. Particle size was determined using LS 13 320 coulter laser diffraction particle size analyzer. In this study, 1% mineral suspension was prepared using drops of sodium hexa-metaphosphate (calgon solution) and deionized water. The content was placed on ultrasonic bath and stirred for 5 minutes. The content was removed from ultrasonic bath, a magnetic base inserted and content stirred for another 5 minutes. Sample was pipetted into the analyzer and run at 8%.

Reactivity Experiments

For reactivity studies to determine the proton coefficient as provided (Eqs. (11), (12), standard laboratory procedure was used [Sparks, 2003, Cavallaro, and McBride, 1978]. 1% single and 1:1 mixed mineral suspensions with no added electrolyte were reacted with solution containing 10ppm of lead regulated to the required pH at the start of experiments. To validate the sorption mechanism involved in lead removal, 1% single and 1:1 mixed mineral suspensions made up to 50 ml were reacted with solution containing 10 ppm of Pb(II) regulated to pH 4. Supernatant was filtered through a cellulose acetate filter (pore size 0.2 μm) and analyzed for Pb(II)), using a Hitachi Atomic Absorption Spectrophotometer (HG-AAS). Sorption of Pb(II) on mineral surfaces requires proton exchange, the stoichiometry of this reaction is described and the proton consumption function is given by:

$$\alpha SOH + M2+ \Rightarrow (SOH)\alpha - M + \alpha H+, \quad (11)$$
$$\log Kd = \log Kp\{SOH\}\alpha + \alpha pH, \quad (12)$$

where SOH is the mineral surface-binding site, M2+ is the soluble metal species, $(SOH)\alpha - M$ is the surface bound metal, logKp is the apparent equilibrium binding constant, and α is the

proton coefficient, representing the number of protons displaced when one mole of metal binds to the mineral surface [[Olivaa, et al., 2011]. Proton coefficient was calculated from the slope of logKd versus pH plot (Fig. 2).

Kinetic Experiments

1% single and 1:1 mixed mineral systems were reacted with solution containing 10ppm of Pb(II) regulated to pH 4. Amounts of Pb(II) remaining in solution after 2, 4, 6, 8, 12, 18, and 24 h were determined using Hitachi Atomic Absorption Spectrophotometer (HG-AAS). Twenty-four hours was sufficient for kinetic studies because sorption reactions occur in milliseconds or minutes [45].

RESULTS

Mineral Systems and Lead Reactivity

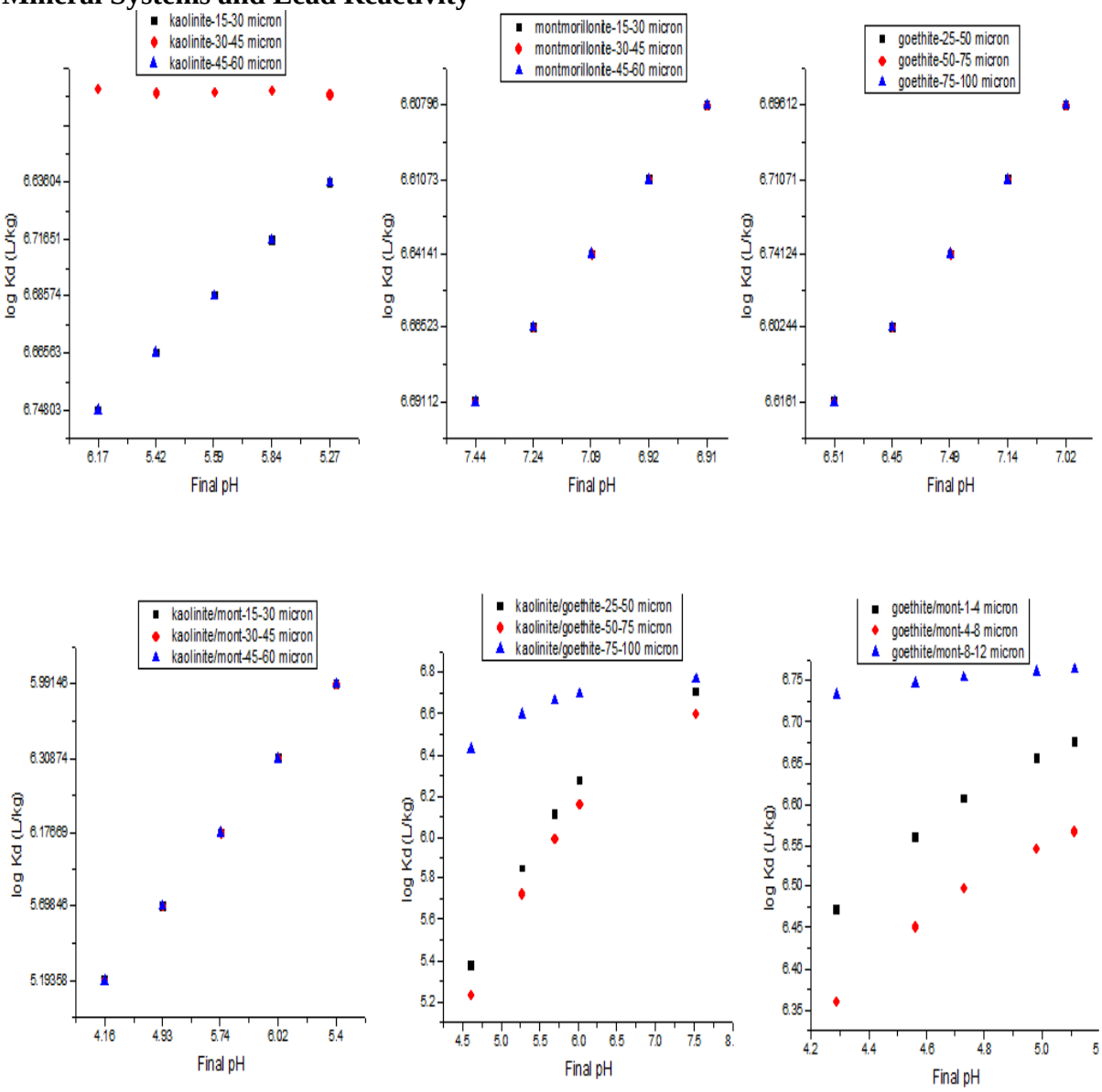

Fig. 1: Plot of Logkd versus Final Ph for Lead Sorbed On Mineral Systems

Table 2: Proton Coefficients (*A*) For Lead Sorbed On Mineral Systems

Mineral	Particle size range (μm)	R-square	α	α_{total}
Kaolinite	15-30	0.99	1.18	n.a
Kaolinite	30-45	0.99	1.16	n.a
Kaolinite	45-60	0.99	1.20	n.a
Montmorillonite	15-30	0.99	0.93	n.a
Montmorillonite	30-45	0.99	0.91	n.a
Montmorillonite	45-60	0.99	0.95	n.a
Goethite	25-50	0.99	0.96	n.a
Goethite	50-75	0.99	0.95	n.a
Goethite	75-100	0.99	0.98	n.a
Kaolinite/montmorillonite	15-30	0.99	1.12	1.05
Kaolinite/montmorillonite	30-45	0.99	1.10	1.04
Kaolinite/montmorillonite	45-60	0.99	1.27	1.07
Montmorillonite/goethite	1-4	0.99	1.05	0.95
Montmorillonite/goethite	4-8	0.99	1.24	0.93
Montmorillonite/goethite	8-12	0.99	1.16	0.96
Kaolinite/goethite	25-50	0.99	1.39	1.07
Kaolinite/goethite	50-75	0.99	1.37	1.06
Kaolinite/goethite	75-100	0.99	1.43	1.07

In this section of the report, n.a means not applicable.

Mineral Systems and Lead Removal Kinetics

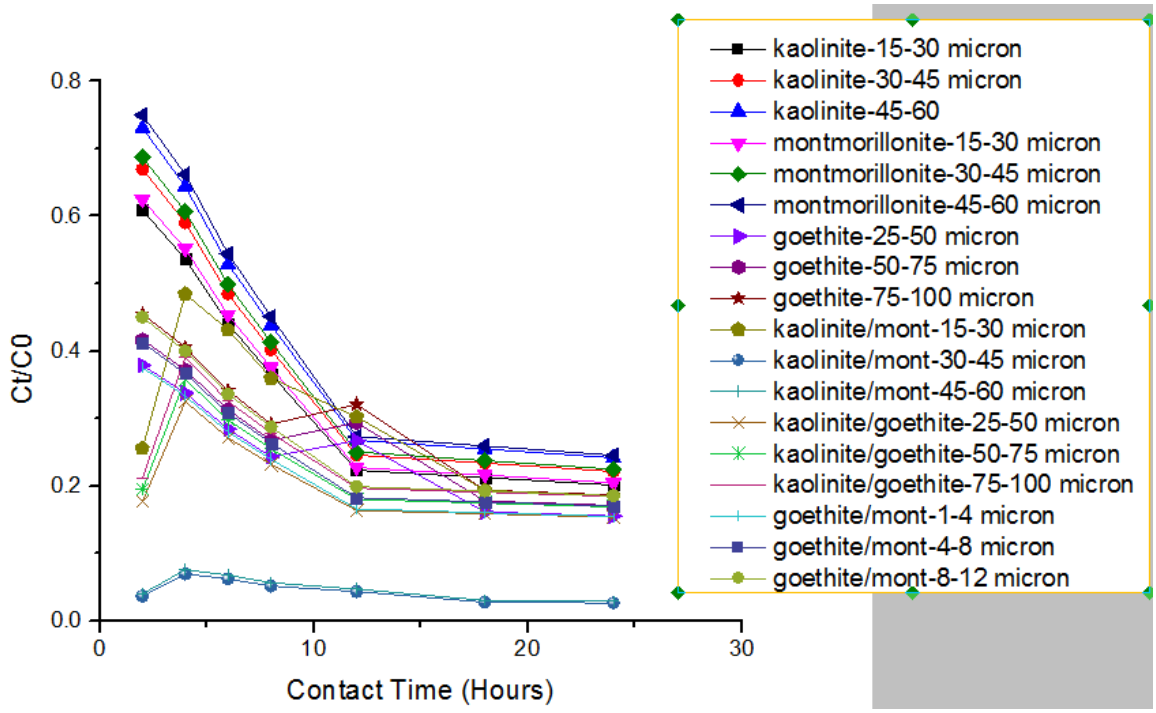

Fig. 2. Plot of Ct/Co versus Residence Time for Lead Sorbed On Mineral Systems

Table 3: Mass Transfer Rates for Lead Sorbed On Mineral Systems

Mineral	Particle size range (μm)	slopeI(hr^{-1})	slopeII(hr^{-1})	Exposed Surface Area (cm^{-1})	K_fI ($cmhr^{-1}$)	K_fII ($cmhr^{-1}$)
K	15-30	0.14	0.013	4700	2.96e-5	2.75e-6
K	30-45	0.15	0.014	4700	3.26e-5	3.03e-6
K	45-60	0.16	0.015	4700	3.55e-5	3.31e-6
M	15-30	0.14	0.013	1000	1.4e-4	1.3e-5
M	30-45	0.15	0.014	1000	1.5e-4	1.44e-5
M	45-60	0.17	0.015	1000	1.7e-4	1.5e-5
G	25-50	0.087	0.096	7100	1.24e-5	1.36e-5
G	50-75	0.096	0.013	7100	1.36e-5	1.95e-6
G	75-100	0.10	0.015	7100	1.48e-5	2.12e-6
KM	15-30	0.091	0.014	8800	1.039e-5	1.65e-6
KM	30-45	0.013	2.1e-3	8800	1.50e-6	2.39e-7
KM	45-60	0.014	2.2e-3	8800	1.64e-6	2.61e-7
MG	1-4	0.086	9.7e-3	14700	5.91e-6	6.62e-7
MG	4-8	0.095	0.010	14700	6.505e-6	7.28e-7
MG	8-12	0.10	0.011	14700	7.09e-6	7.95e-7
KG	25-50	0.061	9.6e-3	7900	7.72e-6	1.22e-6
KG	50-75	0.067	7.9e-3	7900	8.49e-6	1.00e-6
KG	75-100	0.073	0.011	7900	9.26e-6	1.46e-6

In this section of the report, K, M, G, KM, MG and KG represent, kaolinite, montmorillonite, goethite, kaoliniye-montmorillonite, montmorillonite-goethite and kaolinite-goethite respectively.

Table 4: Lead sorbed on mineral systems at pH 4 and 10ppm initial lead concentration

Mineral systems	Particle size range	Mineral systems
Kaolinite	15-30	7.87
Kaolinite	30-45	7.657
Kaolinite	45-60	7.444
Montmorillonite	15-30	7.79
Montmorillonite	30-45	7.569
Montmorillonite	45-60	7.348
Goethite	25-50	7.39
Goethite	50-75	7.129
Goethite	75-100	6.868
Kaolinite/montmorillonite	15-30	7.57
Kaolinite/montmorillonite	30-45	7.327
Kaolinite/montmorillonite	45-60	7.084
Montmorillonite/goethite	1-4	7.75
Montmorillonite/goethite	4-8	7.525
Montmorillonite/goethite	8-12	7.3
Kaolinite/goethite	25-50	5.66
Kaolinite/goethite	50-75	5.226
Kaolinite/goethite	75-100	4.792

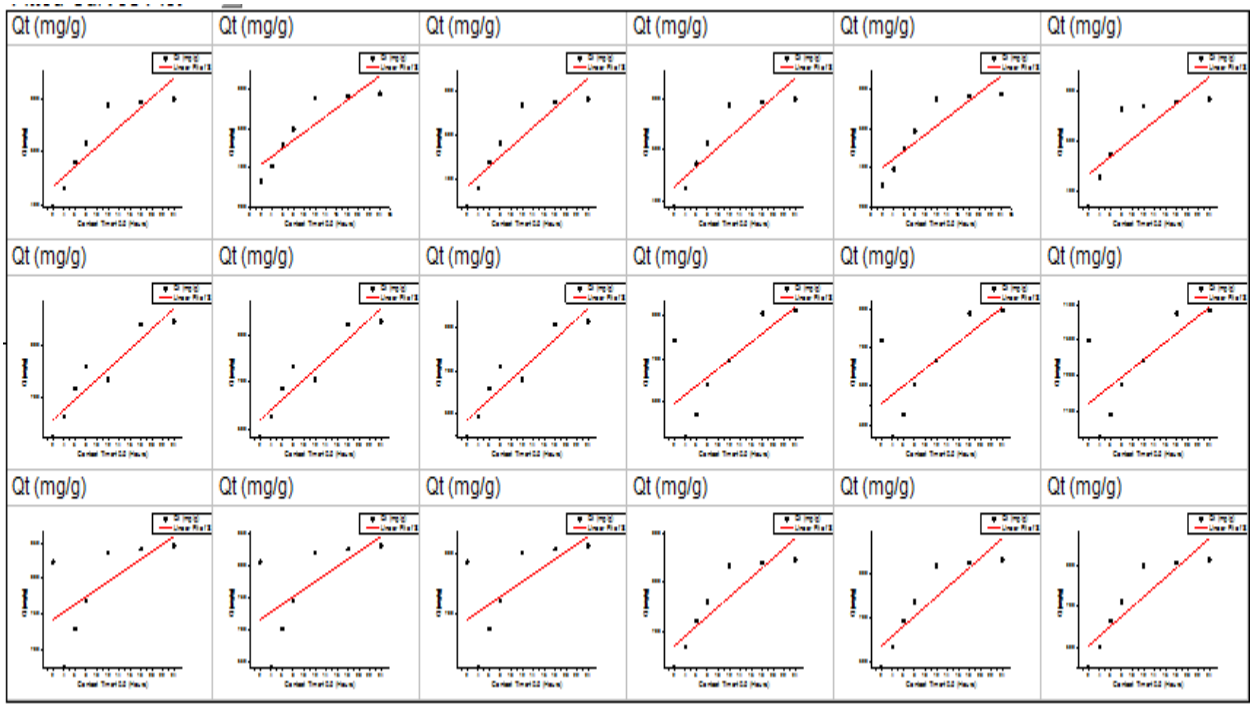

Fig. 3: Fitted Curve Plot Of Sorption Capacity Qt Versus Residence Time T0.5 For Mineral Systems-Represented

Table 5: {Summary of Linear Fit Graphical Analysis for Fig. 3

Mineral	Particle size range (μm)	Ki(Intercept)	C(Slope)	R-Square
Kaolinite	15-30	433.7463	18.57561	0.76224
Kaolinite	30-45	377.12093	20.43317	0.76224
Kaolinite	45-60	320.49556	22.29073	0.76224
Montmorillonite	15-30	417.68285	19.21578	0.76475
Montmorillonite	30-45	359.45114	21.13735	0.76475
Montmorillonite	45-60	433.87517	17.46781	0.59183
Goethite	25-50	635.5563	9.74682	0.84366
Goethite	50-75	599.11193	10.72151	0.84366
Goethite	75-100	562.66756	11.69619	0.84366
Kaolinite/montmorillonite	15-30	575.3422	10.25194	0.7058
Kaolinite/montmorillonite	30-45	532.87642	11.27714	0.74058

Kaolinite/montmorillonite	45-60	7097.41064	12.30233	0.74058
Montmorillonite/goethite	1-4	732.50083	5.26038	0.77833
Montmorillonite/goethite	4-8	705.75092	5.78642	0.77833
Montmorillonite/goethite	8-12	679.001	6.31246	0.77833
Kaolinite/goethite	25-50	650.60297	9.93953	0.75234
Kaolinite/goethite	50-75	615.66327	10.93349	0.75234
Kaolinite/goethite	75-100	580.72357	11.92744	0.75234

TABLE 5: {Summary of Linear Fit Graphical Analysis for Fig. 3

Mineral	Particle size range (μm)	Ki(Intercept)	C(Slope)	R-Square
Kaolinite	15-30	433.7463	18.57561	0.76224
Kaolinite	30-45	377.12093	20.43317	0.76224
Kaolinite	45-60	320.49556	22.29073	0.76224
Montmorillonite	15-30	417.68285	19.21578	0.76475
Montmorillonite	30-45	359.45114	21.13735	0.76475
Montmorillonite	45-60	433.87517	17.46781	0.59183
Goethite	25-50	635.5563	9.74682	0.84366
Goethite	50-75	599.11193	10.72151	0.84366
Goethite	75-100	562.66756	11.69619	0.84366
Kaolinite/montmorillonite	15-30	575.3422	10.25194	0.7058
Kaolinite/montmorillonite	30-45	532.87642	11.27714	0.74058
Kaolinite/montmorillonite	45-60	7097.41064	12.30233	0.74058
Montmorillonite/goethite	1-4	732.50083	5.26038	0.77833
Montmorillonite/goethite	4-8	705.75092	5.78642	0.77833
Montmorillonite/goethite	8-12	679.001	6.31246	0.77833
Kaolinite/goethite	25-50	650.60297	9.93953	0.75234
Kaolinite/goethite	50-75	615.66327	10.93349	0.75234
Kaolinite/goethite	75-100	580.72357	11.92744	0.75234

DISCUSSION

Mineral Systems and Lead Reactivity

The proton coefficient (α) is not characteristic of a particular mineral (Table 2, derived from Figs.1). Differences in α for mixed mineral systems compared to each other and compared to single mineral systems may be linked to differences in the availability of strongly acidic sites All proton coefficient for Pb(II) sorbed on single mineral systems except for goethite are greater than one. This indicated high level of protonation during the sorption process. Proton coefficient for Pb(II)-kaolinite interaction was higher than Pb(II) sorbed on goethite and montmorillonite. This may be attributed to the acidic sites present on kaolinite planar surfaces. Significant numbers of weakly acidic edge sites in goethite and montmorillonite may reduce the proton coefficient because of the limited exchange of protons for sorbing ions. Except for

kaolinite/montmorillonite, mixed mineral suspension, αtotal for Pb(II)sorbed on the mixed mineral suspensions were lower than *α*, indicating attenuated potonation for kaolinite/montmorillonite and enhanced protonation for goethite/kaolinite and goethite/montmorillonite mineral systems. The higher the acidity of sites the more protons are exchanged for Pb(II). Therefore, mineral mixing reduced the acidity of reactive sites for kaolinite/montmorillonite mixed mineral phase. This may be due to the competition for the sorbing ion by the mixed mineral surfaces [3, 34]. The H+/ -M exchange stoichiometry of <2 (Table 2) for Pb(II) sorption on both the single and mixed mineral phases agreed with previous findings [Olivaa, et al., 2011]. This suggested that surface charges became increasingly changed as Pb(II) sorption progressed. In addition, mineral surfaces with few displaceable H+ with limited pH-dependent sorption supported lower H+/ -M stoichiometry.

Mineral Systems and Lead Removal Kinetics

Sorption kinetics indicated a two- phase reaction probably attributed to outer sphere and inner sphere complexation with minimal intra-particle diffusion (Table 3, Fig 3). Mass transfer rate for the first-phase reaction (Kf1) decreased in the order goethite<kaolinite<montmorillonite for all single mineral systems. Mixed mineral systems had a decreasing mass transfer rate for montmorillonite-goethite<kaolinite-montmorillonite< kaolinite-goethite. Theoretical mass transfer rates were higher for kaolinite-montmorillonite and montmorillonite-goethite mixed mineral systems. Kaolinite-goethite exhibited a near similar theoretical KfI value when compared with the actual KfI value.This means that mineral mixing based on empirical model decreased the mass transfer rates for kaolinite-montmorillonite and montmorillonite-goethite, not affecting kaolinite-goethite. For KfII depicting the second-phase reaction, mass transfer rates decreased in the order, goethite<kaolinite<montmorillonite for the single mineral phases. For the mixed mineral systems, the order was, montmorillonite-goethite<kaolinite-goethite<kaolinite-montmorillonite. Based on the empirical model, mineral mixing did not change the mass transfer rates for the mixed mineral systems except for montmorillonite-goethite.

There was a decrease in the mass transfer rate for montmorillonite-goethite. This is because the theoretical mass transfer rate for this mixed mineral system was higher than the actual mass transfer rate. Differences in mass transfer rates for Pb(II) ions transferred to the mineral reactive sites may be attributed (a) to different types of reactive sites on the single and mixed mineral systems (b) differences in BET surface area for the mineral systems [Fig 4] and (c) differences in particle size distribution of these mineral systems. The plot of qt vs. t0.5 was linear and intra-particle diffusion was involved in the sorption process (Fig. 3 and Table 5). However, these lines did not pass through the origin and intra-particle diffusion was not the rate controlling step. This is indicative of some degree of boundary layer control and further shows that the intra-particle diffusion is not the only rate limiting step. This means that other kinetics models may control the rate of lead sorption.

CONCLUSIONS

Lead was investigated to determine particle size effects on its sorption by single and mixed mineral systems of kaolinite, montmorillonite and goethite. This study was in relation to reactivity and kinetics relevant to streams and groundwater impacted by lead. Using empirical models, sorption isotherms indicated that sorption capacities of the different clay minerals, goethite and their mixtures were dependent on the particle size. All proton coefficient for Pb(II) sorbed on single mineral systems except for goethite and montmorillonite are greater than one.

This indicated high level of protonation during the sorption process. All, αtotal for Pb(II) sorbed on the mixed mineral systems were lower than α, indicating enhanced protonation for mineral systems. Mass transfer rate for the first-phase reaction Kf1 were greater than those of the second reaction phase. Mixed mineral systems had a decreasing mass transfer rates. This suggested that different reactive sites were involved in the removal kinetics of the sorbing ions as sorption progressed. Differences in sorption kinetics between the single and mixed mineral phases may be attributed to differences in the BET surface area of single and mixed mineral systems.

ACKNOWLEDGEMENTS

The authors are grateful to the management of Niger Delta University for the release of academic staff allowances. These monies were used for this research work.

Competing Financial Interest Declaration

The authors do not have any conflicting financial interest concerning this project. This project has been funded from academic staff allowances due for the authors.

REFERENCES

Al-Degs, Y.S. Tutunji, M.F. Baker, H.M. (2003). Isothermal and kinetic adsorption behavior of Pb“ions on natural silicate minerals. J. Clay Miner. 38 501–509.

Anagnostopoulos, V. A. Manariotis, I. D. Karapanagioti, H. K Chrysikopoulos, C. V., (2012). Removal of lead from aqueous solutions by malt spent rootlets, Chemical Engineering J. 213, 135–141.

Blesa, M.A. Magaz, v Salfity, J.A. Weisz, A.D. (1997). Structure and reactivity of colloidal metal particles immersed in water. Solid State, 103, 1235–1241.

Brunauer, S. Emmett, P.H. Teller, E. (1938). Adsorption of gases in multimolecular layers, J. Am. Chem. Soc. 60, 309–319.

Cataldo, S., Gianguzza, A., Pettignano, A., Villaescusa, I., (2013). Lead(II) removal from aqueous solution by sorption onto alginate, pectate and polygalacturonate calcium gel beads. A kinetic and speciation based equilibrium study, Reactive & Functional Polymers. 73 207–217.

Cavallaro, N. and McBride, M. B. (1978). Copper and cadmium adsorption characteristics of selected acid and calcareous soils, Soil Sci. Soc. Am. J. 42:550-556.

Crini, G.G. (2005). Recent developments in polysaccharide-based materials used as adsorbents in wastewater treatment, *Prog. Polym. Sci.*, 30(1), 38–70.

Dastoora, AP, Larocpue, Y. (2004). Global circulation of atmospheric lead: a modeling study. Atmos Environ, 38:147–161.

Deshicar, A.M. Bokade, S.S. Dara, S.S., (1990). Modified hardwickia binata bark for adsorption of lead (II) from water, Water Res. 24, 1011–1016.

Dzombak, D.A. Morel, F. Surface Complexation Modeling: Hydrous Ferric Oxide, Wiley, New York, 443-468, 1990.

Egirani, D.E, Baker, A.R, Andrews, J.E. (2005a). Copper and zinc removal from aqueous solution by mixed mineral systems II: The role of solution composition and aging. Journal of Colloid and Interface Science, 291, 326–333.

Egirani, D. E, Baker, A.R, Andrews, J. E. (2005b). Copper and zinc removal from aqueous solution by mixed mineral systems I: Reactivity and removal kinetics Journal of Colloid and Interface Science, 291, 319–325.

Elouear, Z., Bouzid, J., Boujelben, N., Jamoussi, M., Feki, F., Montiel, A., (2008). Heavy metal removal from aqueous solutions by activated phosphate rock, *J. Hazard. Mater*. 156(1), 412–420.

Eric, B. Selma, L., Ronald, L. (2010). Fishing activity, health characteristics and mercury exposure of Amerindian women living alongside the Beni River (Amazonian Bolivia), Inter. J. Hygiene and Environmental Health, 213, 20-40.

Eze, S. O. Igwe, J. C. Dipo, D. (2013). Effect of particle size on adsorption of heavy metals using chemically modified and unmodified fluted pumpkin and broad-leafed pumpkin pods, Int. J. Biol. Chem. Sci. 7(2), 852-860.

Feng, Q. Lin, Q. Gong, F. Sugita, S. Shoya, M. (2004). Adsorption of lead and lead by rice husk ash, J. Colloid and Interface Science, 278, 1–8.

Guedron, S., Cossa, D., Grimaldi, M., Charlet, L., (2011). Methyl-mercury in tailings ponds of Amazonian gold mines (French Guiana): Field observations and an experimental flocculation method for in situ remediation Applied Geochemistry, 26, 222–229.

Hatje, V.H. Hill, D.M. McOrist, G. Birch, G.F. Szymczak, R. (2003). Kinetics of trace element uptake and release by particles in estuarine waters: effects of pH, salinity, and particle loadin J. Environ. Int. 29, 613–618.

Hlavay, J., and Polyak, K. (2005). Determination of surface properties of ironhydroxide-coated alumina adsorbent prepared for removal of arsenic from drinking water. Journal of Colloid and Interface Science, 284, 71–77.

Kitano, Y. Okumura, M. Idogaki, M. (1980). Abnormal behavior of Cu2+ and Zn ions in parent solution at the early stage of calcite formations. Geochem. J. 14 167–175.

Lopez-Mu˜noza, M.J. Aguadoa, J. Arencibiab, A. Pascuala. R. (2011). Lead removal from aqueous solutions of $PbCl_2$ by heterogeneous photo catalysis with TiO_2, Applied Catalysis B: Environmental, 104, 220–228.

Luo, G. Maa, J. Han, J. Yao, H., Xu, M., Zhang, C., Chen, G., Gupta, R., Xu, Z., (2013). Hg occurrence in coal and its removal before coal utilization, Fuel, 104 70–76.

McBride, M.B. (1982). Organic anions adsorption on aluminum hydroxides: spin probe studies, Clay and clay minerals, 30(4), 438-444.

O¨ zcan, A.; O¨ ncu¨, E.M.; O¨ zcan, A.S. (2006). Kinetics, isotherm and thermodynamic studies of adsorption of Acid Blue 193 from aqueous solutions onto natural sepiolite. Colloids and Surfaces A: Physicochemical and Engineering Aspects, 277, 90–97.

Olivaa, J., De Pablob, J., Cortinab, J-L. Camad, J., Ayorad, C., (2011). Removal of cadmium, copper, nickel, cobalt and lead from water by Apatite IITM: Column experiments, Journal of Hazardous Materials, 194, 312–323

Ravenna, L. (1993). Final Burial or Potential Remobilization Water Sci. Technol., 28, 349-358.

Ravichandran, M., (2004). Interactions between lead and dissolved organic matter – a review. Chemosphere, 55, 319–331.

Reichenberg, D. (1952). Properties of ion exchange resins in relation to their structure. III. Kinetics of exchange, J. Am. Chem. Soc. 75, 589–598.

Sparks, D.L (2003). Environmental Soil Chemistry (Ed.). University Press London pp 150-162

Stephan, B. McCarty, K.M. Nadine, S. Beate, L. (2010). Lead exposure and children's health, Current Problems in Pediatric and Adolescent Health Care, 40 186–215.

Strange, E.D and Onwulata, C.I. (2002). Effect of particle size on the water sorption properties of cereal fibers, J. of Food Quality, 25:63-73.

Tan,]. Qiu, Z, Zeng, J. Liu, H. Xiang, H. (2011). Removal of elemental lead by bamboo charcoal impregnated with H_2O_2, Fuel, 90, 1471–1475.

Tombacz, E. Filipcseis, G. Szekeres, M. Gingl, Z. (1999). Particle aggregation in complex aquatic systems J. Colloids Surf. 15 233–244.

Venegas, M. J. Fregoso-Israel, E. Escamilla, R. and Pfeiffer, H. (2007). Kinetic and Reaction Mechanism of CO_2 Sorption on Li_4SiO_4: Study of the Particle Size Effect, Ind. Eng. Chem. Res. 46, 2407-2412.

Wang. Z. Wu, D. Wu, G. Yang, N. Wu, A. (2013). Modifying Fe3O4 microspheres with rhodamine hydrazide for selective detection and removal of Hg2+ ion in water, J. Hazard. Mater. 244– 245, 621– 627.

Zhao, Y, Xue, F., Ma, T., (2013). Experimental study on Hg0 removal by diperiodatocuprate (III) coordinationion solution, Fuel Processing Technology, 106 468–473.